Multi-kilowatt-class heaters for large hollow cathodes

Christopher J. Wordingham,[a),b)] Pierre-Yves C. R. Taunay,[b)] and Edgar Y. Choueiri[b)]
Electric Propulsion and Plasma Dynamics Laboratory, Mechanical and Aerospace Engineering Department, Princeton University, Princeton, New Jersey 08544, USA

(Received 9 March 2018; accepted 17 June 2018; published online 18 July 2018)

Heater materials and geometry are analyzed to address the requirements of large lanthanum hexaboride hollow cathodes. Larger hollow cathodes are capable of increased discharge currents but require higher heater powers to ignite. Existing cathode heaters suffer from material interactions and increased failure rates at high temperatures and are currently not viable for high-power operation; graphite heaters can provide order-of-magnitude increases in heater power and operational life simultaneously. Two models, a simplified circuit model and a finite-element model, were developed to predict the heater operating temperature and resistance. The operational life of the heater was estimated using a vacuum sublimation model. A graphite heater was fabricated and tested using a large-diameter lanthanum hexaboride hollow cathode to demonstrate feasibility as a high-power heater material. The prototype has repeatedly achieved cathode ignition and was tested at up to 4.5 kW of heater power. Heater voltage and current were measured prior to ignition and used to calculate the heater resistance. The measured resistance is within 8% of the predicted value for the circuit model and within 2.5% of the finite-element prediction. At cathode ignition temperatures, the vacuum sublimation model predicts an order-of-magnitude increase in operational life as compared to existing cathode heaters; for a peak surface operating temperature of 1500 °C, the vacuum sublimation model predicts a 1%-loss life of approximately 400 kh. *Published by AIP Publishing.* https://doi.org/10.1063/1.5028392

I. INTRODUCTION

The next generation of high-power Hall thrusters for use in manned and cargo missions is expected to operate at discharge powers ranging from 100 to 200 kW.[1] These thrusters will require cathodes with discharge currents of 300–700 A that can operate for 100 kh,[2,3] outpacing the capabilities of state-of-the-art hollow cathodes. Larger hollow cathodes are candidates for high-power thruster operation but require significantly more heater power to reach emission temperatures.[4]

Hollow cathode heaters are typically manufactured using swaged tantalum with either alumina or magnesium oxide (MgO) insulation.[2,5–8] The electrical resistivity of both materials decreases with increasing temperature,[9] and in the case of MgO, the decrease is so significant as to limit its use to dispenser cathodes operating at temperatures less than 1400 °C.[2] Furthermore, these heaters have the tendency to form voids in the MgO insulation during the swaging process. This can lead to thermal runaway or breakdown failure of the heater insulation, and therefore, thermal cycle testing is required to determine the risk to heater life.[9] Tantalum can also diffuse through and react with the MgO insulation, creating conductive paths that may eventually lead to heater failure.[10] These risks may be further exacerbated by higher-power operation.

Though alumina-insulated heaters have been successfully used for many cathodes and can operate at temperatures between 1600 and 1800 °C depending on the alumina used,[2,8,11] they still face many of the same issues as their MgO-insulated counterparts. These heaters have demonstrated "excellent life" for limited heater currents,[2] but an increase in current of less than 10% of the nominal value can reduce their lifetime to less than 100 h.[8] This sensitivity to operating conditions is also shown in MgO-insulated heaters.[10] The failure mechanisms for alumina-insulated heaters include continued sintering during operation that leads to grain growth and void formation[8] and melting of the heater material during cathode operation due to orifice temperatures exceeding 2000 °C.[5] Neither tantalum nor molybdenum, with melting points of 2996 and 2620 °C, respectively,[12] should be melting at the temperatures reached by the cathode at the heater location. It seems likely that an interaction between the cathode tube and heater materials is at fault. Goebel and Chu propose that the melting is due to Mo–Ta eutectic formation,[5] but this has not been reported in previous work regarding the binary Mo–Ta system.[13–15] Pure alumina does, however, melt at 2050 °C,[12] and the maximum use temperature for alumina is typically restricted to 1750 °C.[11] Commercial additives and grain size refinement can also reduce the melting temperature of alumina to 1700–1850 °C.[12]

The aforementioned problems with swaged heaters occur at power levels much less than a kilowatt, with the highest reported heater power required for operation being approximately 400 W.[6] The anticipated power requirement for larger hollow cathodes is in the multi-kilowatt range[4] due to larger cathode tube diameters and wall thicknesses.

Prior testing of a 2.7 cm inner diameter lanthanum hexaboride (LaB_6) hollow cathode by Plasek *et al.*[4] relied on bare tungsten wire heaters insulated from the cathode tube by boron nitride rings, with or without carbon beads around the tungsten wire to prevent interactions between the wire

[a)]Electronic mail: cjw4@alumni.princeton.edu
[b)]URL: http://alfven.princeton.edu

and the boron nitride. These heaters consistently suffered structural failure due to one or all of the following: arcing or plasma attachment to the heater coil, boride formation, recrystallization embrittlement, localized melting, and possibly even carburization.[4]

McDonald *et al.* have tested a rhenium-wire-based heater enclosed in boron nitride sleeves for high-temperature LaB_6 cathode applications[16] at up to 200 W. The high melting temperature of rhenium, 3185 °C, helps to avoid one failure mechanism, but rhenium forms volatile oxides when exposed to air at temperatures greater than 350 °C, even at reduced pressures.[12] Rhenium is also subject to recrystallization issues.[17]

Recrystallization is one of the primary problems for *any* refractory metal heater and causes the metal to become brittle after exposure to elevated temperatures. Recrystallization begins to take place for tungsten, molybdenum, tantalum, and rhenium at or below 1500 °C.[11,17] The exact temperature at which recrystallization negatively affects a refractory metal part is difficult to determine because it depends on the total time at a given temperature, the degree of cold-working the part has undergone prior to heating, and the presence of any impurities.[17,18] In Ref. 4, temperature measurements of tungsten wire heaters during operation showed that the heater coil was reaching 1800 °C, indicating significant recrystallization of the heater filament. This temperature is beyond the recommended use temperature for alumina, and boron nitride begins to react with bulk tungsten at 1600 °C.[19] Given the tendency of refractory metals for material interactions and degradation of properties at high temperatures, their use in these applications should be avoided.

We have analyzed material interactions and heater geometry to address the shortfalls of refractory metal heaters for high-power heating of large hollow cathodes. We suggest the use of graphite to ensure chemical compatibility with other cathode materials and to remedy the life issues of refractory metals. The use of graphite enables the development of cathode heaters capable of delivering an order-of-magnitude greater power, while prolonging operational life. Section II outlines the analysis of a graphite heater for large hollow cathodes, including materials selection, geometry, and numerical prediction of operating temperature, power, and operational life. We have developed two models to predict the temperature and resistance of the graphite heater: a simplified circuit model and a finite-element model (FEM) using COMSOL multiphysics software. In addition, we have used a vacuum sublimation model to estimate heater life. Following our analysis, we have implemented and tested a graphite heater for a large hollow cathode at input powers of up to 4.5 kW. Experimental results are compared with the numerical predictions in Sec. III.

II. GRAPHITE HEATER ANALYSIS

A. Material considerations

1. Heater element

A graphite cathode heater presents numerous advantages over swaged-tantalum or refractory-wire heaters. The work function of graphite, 5.0 eV, is higher than those of the refractory metals (excluding rhenium),[12,17,20] and it is therefore less likely to act as a secondary cathode during heater operation, discouraging plasma attachment to the heater. The sputtering yield of graphite is also lower than those of both molybdenum and tantalum,[6,20–22] reducing erosion of the heater by the discharge plasma. In vacuum at the temperatures required for large cathode ignition—on the order of 1300–1500 °C[4]—the main life-limiting mechanism for the graphite heater is sublimation rather than melting or chemical interaction. This further prevents shorting of the heater to other cathode components. Graphite is chemically compatible with boron nitride and state-of-the-art hollow cathodes, which rely principally on graphite or molybdenum cathode tubes. Graphite provides a significant advantage over heater architectures that use alumina insulation due to its substantially higher thermal shock resistance,[11,23] possibly allowing for faster cathode ignition. In addition, graphite and boron nitride have similar thermal expansion coefficients in the temperature range of interest.[24] Finally, graphite is lightweight, abundant, and easily machined, and its mechanical properties do not degrade after exposure to high temperatures. Depending on the grade of the material used, graphite becomes stiffer and stronger with increasing temperature.[24] Graphite heaters have also historically been used in other plasma sources, such as that developed by Pongratz and Zöller; in Ref. 25, these authors introduced an "advanced plasma source" (APS) featuring a LaB_6 emitter and a graphite filament heater rated for up to 2.2 kW.[26] These combined characteristics make graphite an attractive material for high-power, long-life heater operation.

2. Electrical leads

The main heater body is connected to the power supply through conductive bars that serve as electrical leads. The material chosen should be electrically conductive and maintain its strength at high temperatures while offering low thermal conductivity to help reduce thermal conduction losses through the electrical leads. Candidate materials for the electrical leads include certain alloys of stainless steel (309, RA253 MA)[27] and titanium carbide.[12] The electrical leads are subsequently connected to copper wiring which is then connected to the heater power supply. This approach prevents direct contact between copper and graphite while maintaining low electrical resistance. At the required operating temperatures, copper would likely melt on contact with the heater tabs, and its thermal conductivity would also increase conduction losses through the electrical leads.

B. Heater geometry

The heater dimensions are chosen to cover the exterior of the cathode tube over the length of the emitter region while sliding over the electrical insulation surrounding the cathode tube. Thermal expansion of the insulation rings is taken into account in the choice of heater inner diameter. Because the cathode tube used is made of the same grade of graphite as the heater, expansion of the cathode tube is not a concern. The flat "pseudo-coil" pattern shown in Fig. 1 of the heater

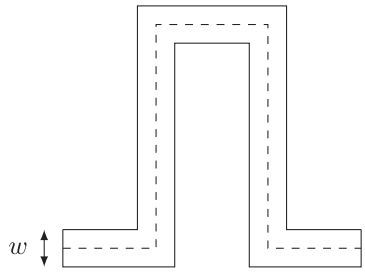

FIG. 1. Pseudo-coil of width w, with thickness t directed into the page. The dashed line indicates the total length, L.

element allows for the appropriate resistance at the desired operating temperature and is simple to machine. This design allows for thermal contact between the heater and the cathode over a large area, and the axial band structure promotes uniform temperature along the length of the cathode tube. A tight fit between the heater inner diameter and the insulation rings covering the cathode tube is not required assuming that adequate radiation heat shielding is used. The number of "coils" was chosen for ease of manufacturing and structural stiffness of the heater bands. A rendering of the corresponding heater with 4 pseudo-coils is shown in Fig. 2. Throughout this paper, we will use the term "band" to refer to the long axial sections of the graphite heater, "tab" to refer to the radial protrusions used as electrical connections, "gap" to refer to the open sections of the heater between bands, and "thickness" to refer to the radial thickness of the heater bands.

This geometry is simple to analyze and can be tailored to fit the desired cathode dimensions and the required heater power; the number of coils along with the band thickness and width can be adjusted freely so long as the heater remains structurally stable.

C. Heater performance

1. Simplified circuit model

Knowledge of the graphite heater resistance is necessary to choose an appropriate power supply for the desired operating temperature. A simplified circuit model can be used to estimate the resistance of the heater at a given operating temperature. If the cathode heat losses are known—estimated using any suitable thermal model of the cathode or prior experiment—then the equilibrium temperature can also be estimated.

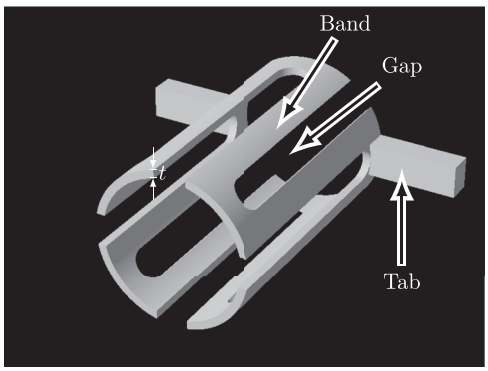

FIG. 2. Computer-aided design rendering of the proposed heater with 4 pseudo-coils and the band thickness, t, indicated.

The resistance and power output of the graphite heater for a given operating temperature T and power supply voltage V_s are estimated with a simplified model that treats each pseudo-coil as a resistor with a constant cross-sectional area—i.e., the variations in cross section at the turning points of the heater bands are ignored. N pseudo-coils (assuming N is even) can then be modeled by two resistors of value R_{half} in parallel, corresponding to the top and bottom halves of the heater, each composed of $N/2$ pseudo-coils. The equivalent resistance of the entire heater, R, is obtained by considering each pseudo-coil as a single resistor of resistance R_{pc} and adding the resulting two resistors of value R_{half} in parallel,

$$R_{\text{half}} = \frac{N}{2} R_{pc}(T) \rightarrow R(T) = \frac{N}{4} R_{pc}(T). \tag{1}$$

Because the cross section of the graphite heater along each coil is assumed constant, each pseudo-coil is modeled as a homogeneous graphite bar of total length L, thickness t, and width w. Hence, R_{pc} is given by

$$R_{pc}(T) = \frac{\rho(T) L}{tw}, \tag{2}$$

where $\rho(T)$ is the resistivity of graphite as a function of temperature.

Assuming that the heater has a uniform temperature and ignoring thermal expansion, we derive a constant "shape factor" from Eqs. (1) and (2) which depends only on geometry:

$$s = \frac{R(T)}{\rho(T)} = \frac{N}{4} \frac{L}{tw}. \tag{3}$$

The heater power delivered at a given temperature and power supply voltage is then readily obtained:

$$P_{\text{heater}} = \frac{V_s^2}{R(T)} = \frac{V_s^2}{s\rho(T)}. \tag{4}$$

The equilibrium temperature can be found by matching the heater power, $P_{\text{heater}}(T)$, with the cathode thermal losses as a function of temperature (which must be obtained via a separate model). We do not use the simplified model to predict equilibrium temperature, only heater resistance.

2. Finite-element approach

We have conducted finite-element simulations of the graphite heater using COMSOL Multiphysics software to obtain the average temperature of the heater for a given input power, the corresponding electrical resistance, and the temperature distribution of the heater along the emitter length. These values are necessary to predict whether cathode ignition can be achieved at a given power and to estimate heater life.

Given the two axes of symmetry of the heater design, we restrict the simulation domain to one quarter of the full 3D geometry. During operation, the heater temperature is expected to be controlled by Joule heating in the graphite and radiation losses from the outward-facing surfaces of the heater element. We impose the following boundary conditions: radiation-to-ambient on the outward-facing surfaces, a potential difference of half the supply voltage between the electrical lead surface

and the vertical symmetry axis, and electrical and thermal insulation on the remaining surfaces. This allows us to predict the current flowing through the heater and the heater temperature. For steady-state operation, we assume that the cathode and the heater have reached thermal equilibrium and that conduction losses to the back of the cathode and electrical leads can be ignored; in this configuration, we need only consider the heat radiated from the outer surfaces. Given that the heater and cathode emitter region temperatures will be similar at steady state, radiative losses to the heat shields are expected to dominate. Thermal and electrical conductivities and surface emissivity as functions of material temperature from Ref. 24 are incorporated into the model. The calculated departure of the temperature from its average value along the cathode length is shown in Fig. 3 for a heater power of 4.7 kW. The mean temperature is 1420 °C.

The bin with the greatest departure from the average temperature, 0–1.02 cm (0–0.4 in.), contains the heater tab which has a temperature well below the mean value. The proposed geometry promotes uniform temperature (and emitter heating) along the cathode axis, with variations that are within 10% of the mean temperature if the tab region is excluded. The maximum temperature of any computational cell is less than 10% greater than the average, and the minimum temperature is approximately 20% less than the average temperature.

D. Lifetime estimation

The machined graphite heater is flexible at room temperature and is ideally only constrained by the electrical leads and cathode tube insulation. Finite-element loading analysis of the heater suggests that it can endure a 6 g sustained axial load and a ±1000 g load applied over 2 ms. This heater would need to undergo a rigorous vibration analysis tailored to the desired launch environment in order to be considered a launch candidate design. Expected thermal stresses are within the fatigue limit of graphite (<50% of ultimate strength),[28] so failure due to thermal cycling is not likely to occur. Previous life tests of hollow cathodes constructed using graphite cathode tubes also suggest that graphite is well-suited to the mechanical and thermal loading inherent in cathode operation.[29]

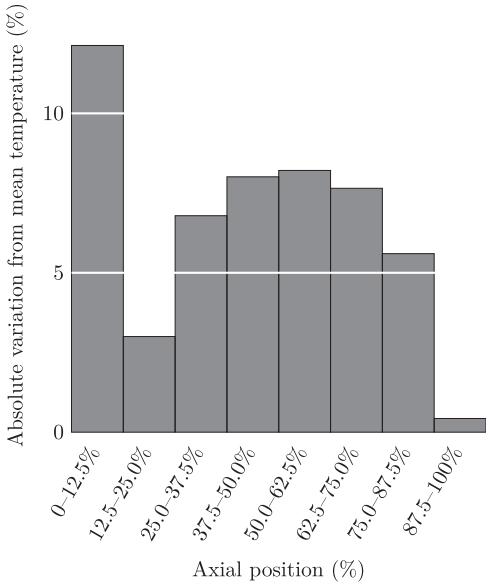

FIG. 3. Axial departure of the FEM-predicted heater temperature from the predicted mean value for a heater power of 4.7 kW (V = 20 V, I = 235 A). The mean temperature is 1420 °C. The total heater length is 8.13 cm (3.2 in.).

The strength and stiffness of the grades of graphite considered increase with temperature.[23,24,30] If the heater can withstand the structural forces it is subjected to while cold, the only likely failure mode is material loss by carbon sublimation. To compute the lifetime of the graphite heater, we rely on vapor pressure data available for carbon at the operating temperatures of interest to calculate the sublimation mass flux of graphite in vacuum.

1. Sublimation mass flux

Though the dominant evaporant species from graphite in vacuum depends on temperature,[31] we assume a worst-case scenario in which atomic carbon is the only species sublimated. The vapor pressure in Torr, P_v, for carbon at temperature T in Kelvin is given by[32]

$$\log_{10} P_v = 16.811 - \frac{37\,940}{T} + 9.64 \times 10^{-4} T - 1.95 \log_{10} T. \tag{5}$$

In the approach outlined in Ref. 33, the upper limit of the mass flux Γ emitted from the heater surface is given by

$$\Gamma = \frac{\rho_g \bar{c}}{4}, \tag{6}$$

where $\bar{c}$ is the average thermal velocity of the evaporating particles and ρ_g is the mass density calculated using the ideal gas law and the vapor pressure from Eq. (5). The average velocity is obtained by assuming a Maxwellian distribution of particles.

A more rigorous approach can be used to estimate the sublimation mass flux with a finite background evaporant pressure, P. Using the experimental data from Ref. 34, we consider a sticking/evaporation coefficient, α_v, equal to unity. The evaporation mass flux Γ from an area A_s at temperature T for a particle of mass m with equilibrium vapor pressure P_v is given by the Hertz-Knudsen law,

$$\Gamma = \frac{1}{A_s}\frac{dm}{dt} = \alpha_v \frac{(P_v - P)}{\sqrt{2\pi m k_B T}} m, \tag{7}$$

where k_B is the Boltzmann constant. Because the heater operates in high vacuum, we assume that the background partial pressure is negligible compared to the equilibrium vapor pressure. In the limit of zero background pressure, Eq. (7) reduces to Eq. (6).

2. Lifetime calculation

The recession velocity v_s of the heater surfaces is subsequently derived from the mass flux per unit area Γ obtained in Eq. (6) or Eq. (7) and the mass density ρ_g of (solid) graphite,

$$v_s = \frac{\Gamma}{\rho_g}. \tag{8}$$

The 1%-loss life of the heater is then calculated using the recession velocity, v_s, and the band thickness, t:

$$\tau_{\max} = t/v_s \cdot 1/100. \tag{9}$$

The 1%-loss life is used because it represents a conservative estimate from an evaporation standpoint and restricts the change in the heater resistance over the heater operational life.

III. RESULTS AND DISCUSSION

Numerical and experimental results are based on the large LaB_6 hollow cathode presented in Ref. 4, which features a 2.7 cm inner diameter, 8 cm long LaB_6 insert and a graphite cathode tube.

A. Implementation

A prototype heater was machined from a solid cylinder of grade AXM-5Q POCO graphite, as delivered from the manufacturer, using a standard manual lathe and milling machine. Figure 4 shows the corresponding machined graphite heater. Table I contains the nominal dimensions of the tested heater. The tabs are electrically connected to two 2/0 copper wires in parallel via four, 1.27 cm wide (1/2-in.) by 0.64 cm thick (1/4-in.) by 15.2 cm long (6-in.) 253MA stainless steel bars. The 253MA stainless steel satisfies the requirements delineated in Sec. II A 2.[27] Each pair of leads is held together with two 1/4 in.-20 bolts to provide good electrical contact with the graphite tabs.

The emitter portion of the cathode tube is insulated by three, 50 μm thick (0.002-in.) molybdenum foil heat shields to reduce radiative losses. While more layers of insulation would be ideal, three layers allow for continued diagnostics access to the heater and cathode tube. Boron nitride insulators enclose the graphite tabs to prevent any electrical connection between the heater and the molybdenum heat shields.

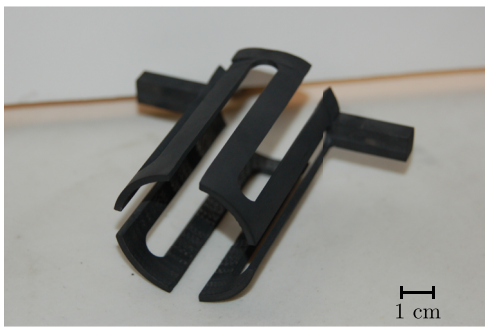

FIG. 4. Finished graphite heater.

TABLE I. Nominal dimensions of the heater.

Dimension	cm (in.)
Axial length	8.13 (3.20)
Inner diameter	4.45 (1.75)
Outer diameter	4.95 (1.95)
Band width	0.91 (0.360)
Band thickness	0.25 (0.100)
Gap width	1.00 (0.394)
Tab length	2.54 (1.00)
Tab width	0.76 (0.300)
Tab height	1.00 (0.394)

The final setup without molybdenum heat shields is shown in Fig. 5(a).

B. Experimental results

1. Apparatus and procedure

The heater is powered by an American Reliance 32 V/400 A power supply. The cathode and heater are installed in a 2 m diameter by 5 m long vacuum vessel evacuated to less than 8×10^{-5} Torr. Pressures in this range should ensure both negligible convection losses and negligible impact on graphite sublimation. Temperature measurements were taken during cathode heating using a type C thermocouple installed on the outer radial surface of the cathode tube tip and a Leeds & Northrup Model 8622-C optical pyrometer aimed manually at the exposed portion of the heater tip as indicated in Fig. 5(b) from a distance of approximately 1 m. To characterize the heater, we varied the heater current in 25 A increments and let the heater reach steady state at each operating point with no gas flow through the cathode. Pyrometer and thermocouple readings were taken after 10–20 min when the heater reached a stable temperature. The heater voltage was measured simultaneously using an NI 9206 data acquisition system and a 4:1 voltage divider. Heater current data were taken from the digital set point of the power supply. To avoid subjective bias in the pyrometer measurements, two readings were taken, each by a different observer, and subsequently averaged. Temperatures below 760 °C are outside the range of our optical pyrometer.

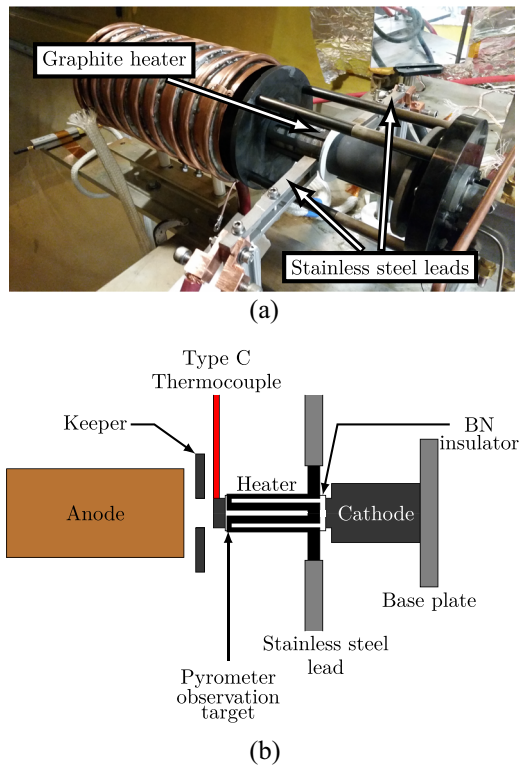

FIG. 5. Installed graphite heater and equivalent experimental schematic. (a) Graphite heater installed on the hollow cathode without heat shields. (b) Equivalent schematic.

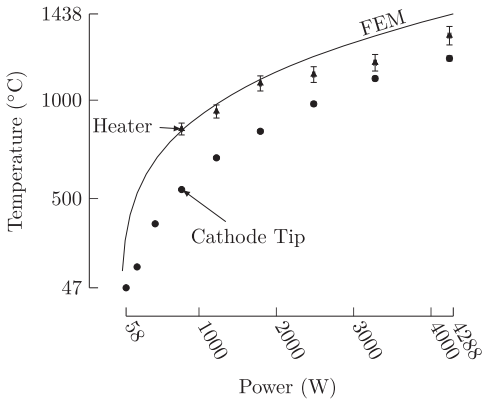

FIG. 6. Measured cathode tip and heater element temperatures versus heater power. The surface-averaged heater temperatures predicted by the FEM are also shown versus the input power.

2. Operating temperature

Thermocouple and optical pyrometer data are shown with the calculated surface-averaged temperatures from the finite-element model in Fig. 6 versus heater power. The results of the finite-element model agree qualitatively with the pyrometric data, but the model overpredicts the heater temperature for high powers. This may be due to the exclusion of conduction losses through the cathode tube and electrical leads in the finite-element model. The agreement between the finite-element results—without heat shielding—and the heater pyrometer data suggests that significant thermal losses are present in the prototype cathode.

3. Heater resistance

The predicted heater resistances from the circuit and finite-element approaches are shown in Fig. 7. Heater resistance calculated from the experimental voltage and current data is also shown versus the measured heater temperature.

Experimental heater resistance follows the same trend as the circuit and finite-element model predictions; the resistance decreases with increasing temperature below 500–750 °C and then increases approximately linearly with temperature. This is not visible in the heater pyrometer data, but because the cathode temperature is not representative of the heater temperature, we cannot use it for quantitative predictions. The circuit model underestimates the experimental resistance data by less than 8% and excludes the resistance of the heater tabs. In order to properly include the tab resistance an estimate of the current distribution would be necessary. The finite-element model provides an improved estimate of the heater resistance with the experimental resistance measurements within 2.5% of the predicted values.

C. Lifetime estimation

The 1%-loss life of the heater with the dimensions given in Table I calculated using the approach delineated in Sec. II D is shown in Fig. 8. We predict a lifetime of approximately 400 kh for a graphite heater with the specified geometry operating continuously at 1500 °C. Based on the measured heater temperature of 1328 °C and the observation from the finite-element model that the temperature of the heater tip should be within about 10% of the peak surface temperature, we do not expect the temperature of any portion of the heater surface to exceed 1500 °C. Considering that this operational life is a conservative estimate, this heater architecture is promising for long-term missions.

D. Limitations

The graphite heater element itself could process up to 11 kW with the power supply available, but our measurements are currently limited to 4.5 kW. This limitation is due to the melting of the steel electrical leads at input currents above 230–240 A. We can ignite the cathode in a repeatable fashion using the heater in its current form; reduction in the required power by improved shielding is still desirable. Removing the temperature limitation imposed by the electrical leads would demonstrate that this heater architecture is suitable for even higher power operation. Titanium carbide leads may alleviate melting issues, with a melting point of over 2940 °C,[12] but stainless steel is expedient and inexpensive. We have also found that placing molybdenum foil around the graphite tabs distributes heat at the contact surface and prevents bonding/melting between the graphite and the steel leads without introducing significant thermal losses. Other refractory carbide materials may also provide satisfactory replacements for

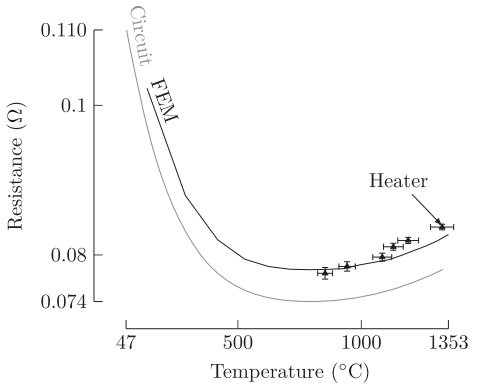

FIG. 7. Heater resistance versus temperature, calculated using the circuit model, finite-element model, and experimental I-V measurements.

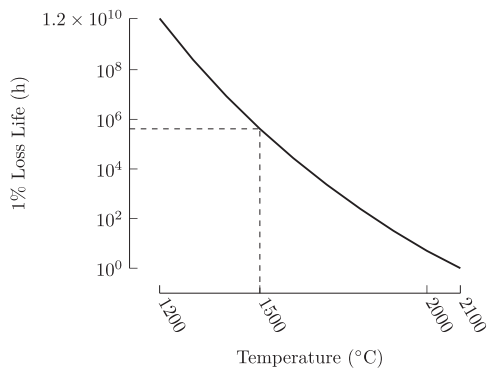

FIG. 8. Estimated heater lifetime as a function of operating temperature. Time required for sublimation of 1% of the heater band thickness.

the electrical leads. Pure refractory metals are prone to failure as described in Sec. I, but refractory carbides do not exhibit the same problems and do not react with graphite at high temperatures in vacuum.[35]

IV. CONCLUSION

We have conducted an analysis of heater materials and geometry to address the needs of large thermionic hollow cathodes. Graphite presents a possible solution to both increase heater power and alleviate life issues facing swaged-tantalum and refractory-metal heaters during high-power operation. To predict graphite heater operating temperature and resistance, we have developed a simplified circuit model and a finite-element model. We estimate heater life using a vacuum sublimation model.

Following our analysis, we developed a prototype graphite heater. Ignition of a 2.7 cm inner diameter lanthanum hexaboride hollow cathode was achieved in a repeatable fashion using the prototype heater. We operated the heater at up to 4.5 kW of input power, achieving a temperature of 1328 °C as measured on the exposed surface of the heater element by optical pyrometry. Higher heater power could be achieved by replacing the stainless steel electrical leads with refractory carbide materials; the only current limitation is localized melting of the electrical leads. No other degradation of heater performance has been detected. Measured heater resistance values were within 8% of the values predicted by the simple circuit model and 2.5% of those predicted by the finite-element model. The principal predicted heater-life-limiting mechanism is reduction of the element thickness by carbon sublimation, and for the measured temperature of the exposed heater surface, the peak surface temperature is not expected to exceed 1460 °C. We estimate a 1%-material-loss life of 400 kh—over 40 years of continuous operation—at 1500 °C.

Graphite heaters can be used for a wide range of cathode sizes, eliminating the material problems encountered in existing heater designs and allowing for an order-of-magnitude increase in available heater power and operational life.

ACKNOWLEDGMENTS

This work was supported by the U.S. Air Force Office of Scientific Research under Grant No. FA9550-11-1-0241. We would also like to thank Bob Sorenson for his technical support.

[1]D. L. Brown, B. E. Beal, and J. M. Haas, in *IEEE Aerospace Conference* (IEEE, 2009).
[2]D. M. Goebel and E. Chu, in International Electric Propulsion Conference, 2011, IEPC-2011-053.
[3]R. R. Hofer, T. M. Randolph, D. Y. Oh, J. S. Snyder, and K. H. de Grys, in Joint Propulsion Conference, 2006.
[4]M. L. Plasek, C. J. Wordingham, S. Rojas Mata, N. Luzzaraga, E. Y. Choueiri, and J. E. Polk, in Joint Propulsion Conference, 2014.
[5]D. M. Goebel and E. Chu, J. Propul. Power **30**, 35 (2014).
[6]E. Chu, D. M. Goebel, and R. E. Wirz, J. Propul. Power **29**, 1155 (2013).
[7]D. M. Goebel and E. Chu, in Joint Propulsion Conference, 2012.
[8]D. M. Goebel and R. M. Watkins, Rev. Sci. Instrum. **81**, 083504 (2010).
[9]A. Mathers, in Joint Propulsion Conference, 2008.
[10]W. G. Tighe, K. Freick, and K.-R. Chien, in Joint Propulsion Conference, 2005.
[11]See http://www.thermoshield-us.com/pdf/Copy-of-material-properties-chart-w-Ceramics.pdf for Thermo-Shield, "Typical properties of materials," 2015.
[12]F. Cardarelli, *Materials Handbook*, 2nd ed. (Springer, 2008).
[13]J. J. English, "Binary and ternary phase diagrams of columbium, molybdenum, tantalum, and tungsten," Technical Report 152, Defense Metals Information Center, 1961.
[14]E. Rudy, "Ternary phase equilibria in transition metal-boron-carbon-silicon systems," Technical Report AFML-TR-65–2, Air Force Materials Laboratory, 1969.
[15]W. Xiong, Y. Du, Y. Liu, B. Y. Huang, H. H. Xu, H. L. Chen, and Z. Pan, CALPHAD: Comput. Coupling Phase Diagrams Thermochem. **28**, 133 (2004).
[16]M. S. McDonald, A. D. Gallimore, and D. M. Goebel, Rev. Sci. Instrum. **88**, 026104 (2017).
[17]E. M. Savitskii and G. S. Burkhanov, *Physical Metallurgy of Refractory Metals and Alloys* (Consultants Bureau, 1970).
[18]H. E. Patee and R. M. Evans, "Brazing and bonding of columbium, molybdenum, tantalum, tungsten, and graphite," Technical Report 153, Defense Metals Information Center, 1962.
[19]E. Lassner and W. Schubert, *Tungsten* (Springer Science+Business Media, LLC, 1999).
[20]D. R. Lide, *Handbook of Chemistry and Physics*, 77th ed. (CRC Press, 1997).
[21]M. A. Mantenieks, J. E. Foster, K. R. Pradosh, S. V. Shutthanandan, and T. S. Thevuthasan, in International Electric Propulsion Conference, 2001, IEPC-2001-309.
[22]R. P. Doerner, D. G. Whyte, and D. M. Goebel, J. Appl. Phys. **93**, 5816 (2003).
[23]Entegris, "Properties and characteristics of graphite" (2013), https://www.entegris.com/content/dam/web/resources/brochures/brochure-properties-and-characteristics-of-graphite-7329.pdf.
[24]Poco Graphite, Inc., "Properties and characteristics of graphite for industrial applications" (2015), http://www.poco.com/Portals/0/Literature/Semiconductor/IND-109441-0115.pdf.
[25]S. Pongratz and A. Zöller, J. Vac. Sci. Technol., A **10**, 1897 (1992).
[26]J. Harhausen, R. P. Brinkmann, R. Foest, M. Hannemann, A. Ohl, and B. Schröder, Plasma Sources Sci. Technol. **21**, 035012 (2012).
[27]Rolled Alloys, "RA 253 MA data sheet," 2012, http://content.rolledalloys.com/technical-resources/databooks/RA253MA_DB_US_EN.pdf.
[28]S. Ishiyama, T. Oku, and M. Eto, J. Nucl. Sci. Technol. **28**, 472 (1991).
[29]Y. Ohkawa, T. Higuchi, Y. Hayakawa, K. Miyazaki, and H. Nagano, in International Electric Propulsion Conference, 2013, IEPC-2013-364.
[30]Poco Graphite, Inc., "Properties and characteristics of graphite for the EDM industry" (2002), http://www.poco.com/Portals/0/EDM/Properties%20and%20Characteristics%20of%20Graphite%20for%20the%20EDM%20Industry.pdf.
[31]P. D. Zavitsanos and G. A. Carlson, J. Chem. Phys. **59**, 2966 (1973).
[32]R. Setton, *Carbon Molecules and Materials* (CRC Press, 2002).
[33]P. Thieberger, "Upper limits for sublimation losses from hot carbon targets in vacuum and in gases," Technical Report MUC-0186, Brookhaven National Laboratory, 2000, www-mucool.fnal.gov/mcnotes/public/pdf/muc0186/muc0186.pdf.
[34]B. Paul, ARS J. **32**, 1321 (1962).
[35]A. L. Burykina and T. M. Evtushok, Powder Metall. Met. Ceram. **3**, 104 (1964).